

RESEARCH ON THE ADSORPTION OF Pb^{2+} BY APATITE ORE AND PURIFIED APATITE ORE

Nguyen Thu Phuong^{1,*}, Cao Thi Hong^{1,2}, Nguyen Thi Thuy³, Nguyen Thi Xuyen¹,
Nguyen Thi Thom¹, Pham Thi Nam¹, Nguyen Thi Thu Trang¹, Do Thi Hai⁴,
Dinh Thi Mai Thanh^{1,5,*}

¹*Institute for Tropical Technology, Vietnam Academy of Science and Technology,
18 Hoang Quoc Viet, Cau Giay, Ha Noi, Viet Nam*

²*Graduate University of Science and Technology, Vietnam Academy of Science and Technology,
18 Hoang Quoc Viet, Cau Giay, Ha Noi, Viet Nam*

³*Vietnam Institute of Industrial Chemistry, 2 Pham Ngu Lao, Hoan Kiem, Ha Noi, Viet Nam*

⁴*Hanoi University of Mining and Geology, 18 Pho Vien, Bac Tu Liem, Ha Noi, Viet Nam*

⁵*University of Science and Technology of Hanoi, Vietnam Academy of Science and Technology,
18 Hoang Quoc Viet, Cau Giay District, Ha Noi, Viet Nam*

*Emails: 1.ntphuong@itt.vast.vn, 2.dtmthanh@itt.vast.vn

Received: 20 March 2021; Accepted for publication: 24 August 2021

Abstract. Apatite ore from Lao Cai province (Viet Nam) has large reserves and low cost which was purified by a simple chemical method. Apatite ore and purified one were characterized for their molecular structure, phase component, specific surface area, element component, and morphology by Infrared (IR), X-ray Diffraction (XRD), Brunauer-Emmett-Teller (BET), Energy Dispersive X-ray (EDX), and Scanning Electron Microscope (SEM) methods. The IR results show that both materials have functional groups of fluorapatite such as PO_4^{3-} and F^- . XDR and EDX confirm that the main component of the ore is fluorapatite. After purification, the particles are smaller and more uniform with a higher specific surface area ($36.62 \text{ m}^2/\text{g}$ compared with $3.76 \text{ m}^2/\text{g}$ of the original apatite ore). Two materials were used to adsorb Pb^{2+} ions from an aqueous solution. The effect of adsorbent mass, pH, Pb^{2+} initial concentration, and contact time on adsorption efficiency and capacity was evaluated. The study of adsorption kinetics and isothermal adsorption showed that the Pb^{2+} adsorption process on apatite ore is in good agreement with the pseudo-second-order kinetic model and the Langmuir model. The zeta potential and phase structure of apatite ore before and after Pb^{2+} adsorption were investigated. A comparison between the original apatite ore and purified one was also made. With 0.05 g of adsorbent, after 15 minutes, the efficiency of purified ore is 97.47 %, much higher compared with the original ore (50 %) after 45 minutes.

Keywords: Apatite ore, purified apatite ore, adsorption, Pb^{2+} ions.

Classification numbers: 3.4.2, 3.6.1, 3.7.3

1. INTRODUCTION

Heavy metals are natural components of the earth's crust, but human activities in the process of industrialization have made environmental pollution caused by heavy metals, especially the contamination of water environment becomes more and more serious. Heavy metals can accumulate in the environment and ecosystem, both in surface water and groundwater. They can follow the food chain and affect human health and animals [1,2]. Particularly, lead (Pb), a very toxic metal, is released to the environment due to its wide use in many industries such as metallurgy, storage battery, printing, electronics, ammunition, products and pipes made by copper, ceramic and glass industry [3]. Lead can affect the nervous, circulatory, and skeletal system, anemia, anorexia, vomiting, and increase blood pressure, stomach pain, brain and kidney damage, osteoporosis [3, 4]. According to WHO, the lead limit is 0.05 mg/L [3].

Different methods are used for heavy metal treatment such as ion exchange, chemical precipitation, coagulation, electro-coagulation, flocculation, membrane separation, reverse osmosis, and adsorption [1-3]. In particular, the adsorption method is widely used because of its simple design, easy operation, high efficiency even at low concentrations, and low cost [1, 3]. Many materials were used to adsorb heavy metals such as commercially adsorbents (graphene, activated carbon, carbon nanotube - but they are expensive), natural materials (clays, zeolites, siliceous material), bio-adsorbents, waste materials [3], and synthetic materials such as silica [4], zirconium-based ferromagnetic [1], and apatite. Apatite comes in 3 forms: hydroxyapatite ($\text{Ca}_{10}(\text{PO}_4)_6(\text{OH})_2$), fluorapatite ($\text{Ca}_{10}(\text{PO}_4)_6\text{F}_2$), and chlorapatite ($\text{Ca}_{10}(\text{PO}_4)_6\text{Cl}_2$), of which hydroxyapatite is the main component of bone and teeth and was synthesized to treat many toxic inorganic and organic compounds such as dyes (methylene blue [2,5], acid yellow 220, Congo red, reactive blue 19, methyl orange [5]), F^- [6], some emerging pollutants such as cosmetics, herbicides, pharmaceutical [5] and heavy metals such as Pb^{2+} [5,7], Cu^{2+} [5,8], Cd^{2+} [5, 8, 9], As (V), Cr(VI), Cs^+ , Zn^{2+} [5]. Both fluorapatite and chlorapatite are minerals that exist in natural ores. In the world, apatite ore was used to treat heavy and radioactive metals in soil and groundwater due to its huge reserves, low cost, high efficiency, and simple process under different names such as in-situ remediation techniques, phosphate-induced metal stabilization. Apatite can adsorb Cu, As, Zn, Th, Ac, U, Pu, Sr, Cd, Se, Cs, Tc, and Pb ions [10 - 16] and prevent water pollution. Heavy and radioactive metal ions can react with PO_4^{3-} to form a precipitate and can displace calcium ions in the structure of apatite [14].

In Viet Nam, apatite ore in Lao Cai province has the main component of fluorapatite with a huge amount of 2550 million tons which is mainly used to fabricate fertilizer [8]. The adsorption capacity of this material has not been investigated much and there were only a few publications about the initial ore [19, 20].

In this study, apatite ore was purified by the chemical method in order to remove some impurities in the ore, which is a new finding of this research compared with other studies in Viet Nam [19, 21, 22]. Then, the apatite ore and purified one were characterized for their properties using methods such as IR, SEM, XRD, BET, EDX. After that, the apatite ore was used for lead ion adsorption. The effect of factors such as mass, pH, contact time, Pb^{2+} concentration was investigated, and adsorption isotherm was determined. The zeta potential and phase structure of apatite ore before and after Pb^{2+} adsorption were studied. A comparison between apatite ore and purified one in terms of Pb^{2+} adsorption capacity was made.

2. MATERIALS AND METHODS

2.1. Materials

Apatite ore is from Lao Cai, Viet Nam. NaOH 96 %, KCl 99.5 %, NaCN 98 %, HCl 36 %, NH₃ 25 %, Chlorofom 99 % are pure chemicals from China; Pb(NO₃)₂ 99.5 % and Dithizone 98 % are pure Merck chemicals.

Purification experiment: Apatite ore from Lao Cai, Viet Nam was milled and dried at 100 °C in an oven. After that, it was purified by the following procedure: apatite ore was dispersed in water and stirred at room temperature at a rate of 400 rpm. And then, HCl solution (HCl: H₂O = 1:4 (V:V)) was gradually added to the above solution and was continuously stirred for 1 hour. The obtained powder was filtered and rinsed by distilled water to a pH value of 7. After that, 8 % NaOH solution was added to the powder and was boiled at 100 °C for 7 hours. The solution was cooled down to room temperature, the powder was filtered and rinsed by distilled water to pH 7, and was dried at 100 °C.

2.2. Methods

The molecular structure of apatite ore and purified apatite ore was characterized by Infrared (IR, Nicolet iS10, Thermo Scientific). The morphology and element components were determined by Scanning Electron Microscope - Energy Dispersive X-ray spectroscopy (SEM-EDX, SM-6510LV, Jeol-Japan, X-Act, Oxford Instrument-England). The phase component was examined by X-ray Diffraction (XRD, D8 ADVANCE-Bruker, CuK_α radiation ($\lambda = 1.54 \text{ \AA}$) with a step angle of 0.030°, scanning rate of 0.0428 s⁻¹, and 2 θ degree in the range of 10-70°). And the specific surface area was determined by Brunauer-Emmett-Teller methods (BET, TriStar II, Micromerit, 77K, N₂). The zeta potential of apatite ore before and after Pb²⁺ adsorption was measured by the Dynamic Light Scattering method (DLS, SZ-100V2, Horiba Scientific, Japan) in the charge range of -200 to 200 mV at 25 °C.

2.3. Adsorption experiments

The Pb²⁺ ion adsorption experiments were conducted with 50 mL of Pb(NO₃)₂ solution in the range of concentration from 10 mg/L to 100 mg/L. A content of apatite ore (from 0.05 g to 0.4 g) and purified apatite ore (from 0.005 g to 0.1 g) was introduced into the Pb(NO₃)₂ solution. The initial pH of the solution was adjusted from 4 to 8 using 0.01 M NaOH and 0.01 M HCl, measured with a pH meter (1100H VWR pHenomenal - Germany). By using a magnetic stirrer (Velp Scientifica) at a rate of 400 rpm, the mixture was stirred for various periods of time (15, 30, 45, 60, and 70 minutes). After the adsorption process, the Pb²⁺ concentration in the solution was determined by UV-vis with a complex of Pb²⁺ and dithizone or by AAS method. The UV measurements were conducted by UV-Spectrometer, CINTRA40-USA. The Pb²⁺ concentration was also determined by AAS method at a wavelength of 217 nm on AAS iCE 3500 Thermo Scientific (Germany).

Dithizone (diphenylthiocarbazon) is an organic reagent that can make a complex with Pb²⁺ ions. The Pb-dithizonate complex has a red color and is dissolved in organic solvent chloroform. This color complex has a peak at the wavelength of 520 nm. Pb-dithizonate was extracted from solution at pH = 8 - 9, containing the residual CN⁻ which was used to complex with other metal ions.

Pb²⁺ adsorption efficiency H (%) and capacity Q (mg/g) were calculated by the following equations:

$$H = (C_o - C_e) \cdot \frac{100}{C_o} \quad (1)$$

$$Q = (C_o - C_e) \cdot \frac{V}{m}$$

where C_o (mg/L) is the initial Pb^{2+} concentration in the solution, C_e (mg/L) is the equilibrium Pb^{2+} concentration after the adsorption process, V (L) is the solution volume ($V = 50$ ml), and m (g) is the mass of apatite ore or purified one.

3. RESULTS AND DISCUSSION

3.1. Characterization of apatite ore and purified apatite ore

3.1.1. IR spectrum.

Figure 1 shows the IR spectra of Lao Cai apatite ore and purified one. The characteristic peaks for vibration of PO_4^{3-} were observed at 1097, 1046, 600, 564, and 469 cm^{-1} . In which, asymmetric stretching vibration of P-O was characterized by 2 peaks: 1097 and 1046 cm^{-1} . The asymmetric bending vibration of O-P-O was observed at 600 and 564 cm^{-1} . Adsorption peaks with strong intensity at a wavenumber of about 3417 cm^{-1} correspond to the stretching vibration of OH^- or adsorbed water, besides, the bending vibration of OH^- group is characterized by peaks with a wavenumber of about 1617 cm^{-1} . The peak at 696 cm^{-1} in the range from 674 and 720 cm^{-1} was attributed for F^- [17]. Apart from that, there are peaks at 1458 and 1426 cm^{-1} that belong to the vibration of CO_3^{2-} [18]. IR spectra show that the apatite ore and purified one have PO_4^{3-} and F^- groups of fluorapatite molecular $Ca_{10}(PO_4)_6F_2$.

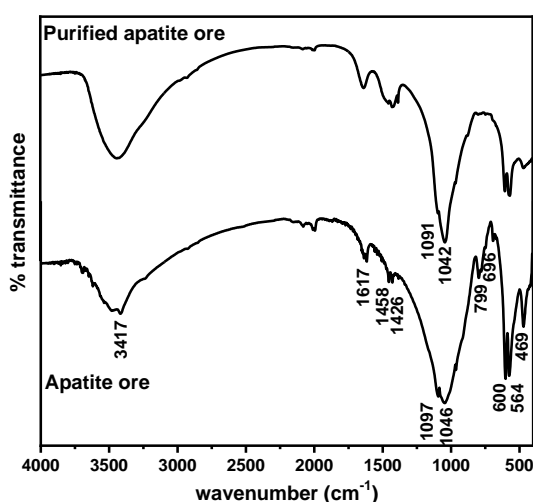


Figure 1. IR spectra of apatite ore and purified apatite ore.

3.1.2. Scanning electron microscopy (SEM)

The morphology of apatite ore before and after modification was presented in Figure 2. It can be observed that the apatite ore particles have an ununiform size. The large particles can reach 15 - 20 μm in size and the smallest particles have a size of about 200 nm (Figure 2.a). After purification, the particles have a more uniform and smaller size than the original apatite ore (Figure 2.b). Furthermore, the particles after purification are more porous, leading to a possible increase in the specific surface area and the adsorption capacity of the material, which will be shown in the next parts.

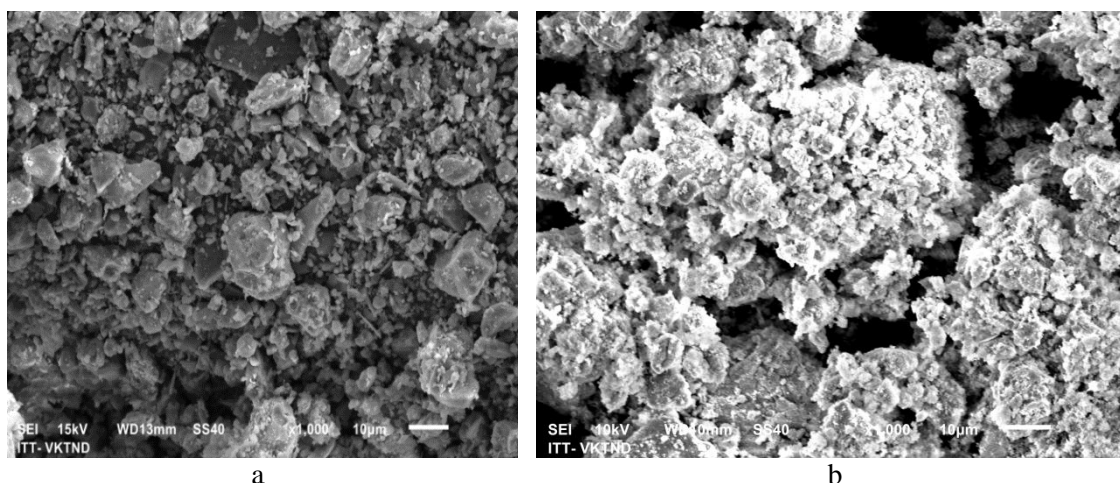


Figure 2. SEM images of apatite ore (a) and purified apatite ore (b).

3.1.3. X-ray diffraction pattern (XRD)

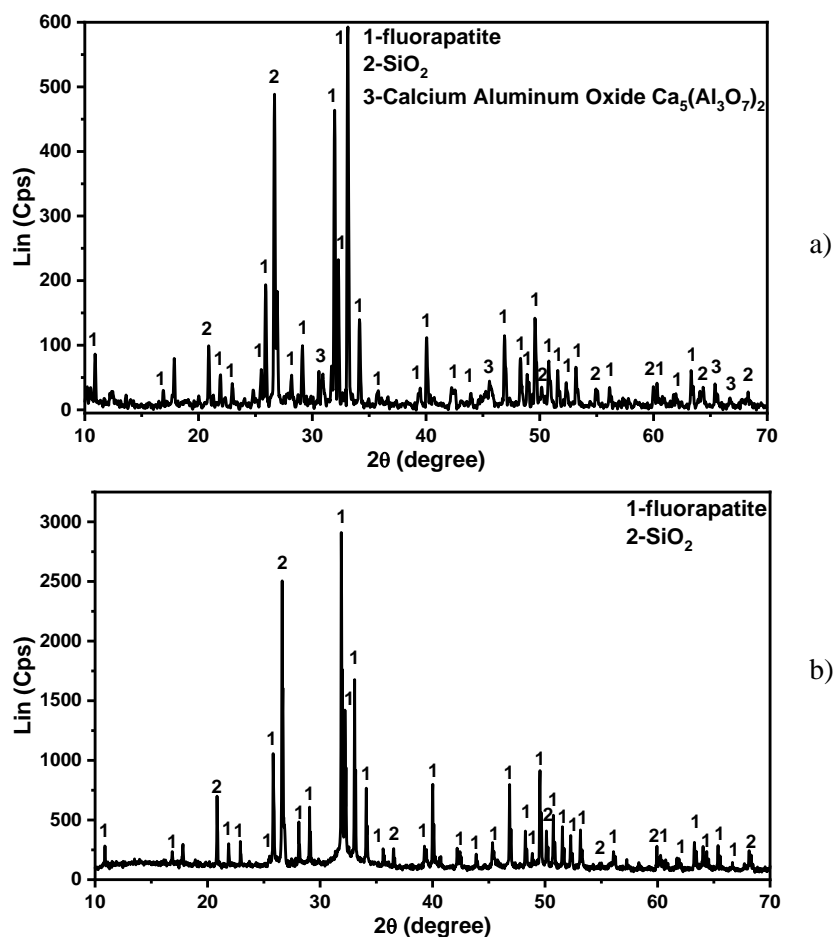


Figure 3. X-ray diffraction pattern of apatite ore (a) and purified apatite ore (b).

The apatite ore and purified one were studied by X-ray diffraction method to specify the crystallinity and phase component of the adsorbent materials (Figure 3). These characteristic peaks of the fluorapatite phase and some other peaks corresponding to SiO₂ and Ca₅(Al₃O₇)₂ were observed in the pattern of apatite ore. The diffraction peaks of fluorapatite phase Ca₁₀(PO₆)F₂ are at 2θ values of about 32°; 33°; 34°. Besides, some other peaks with lower intensity at 2θ of about 11°; 26°; 36°; 40°; 47°; 50°, etc. [PDF 00-015-0876, 18] were observed. The peaks at 2θ values of about 21° and 26.7° are corresponding to SiO₂ [PDF 00-046-1045]. The peak of Ca₅(Al₃O₇)₂ is at 2θ of about 31° [PDF01-070-0801]. The above results indicate that the crystal phase component in apatite ore contains mainly fluorapatite and a small amount of SiO₂ and Ca₅(Al₃O₇)₂. For purified apatite ore sample (Figure 3.b), only peaks characterized for fluorapatite and SiO₂ are observed. This proves that the purification process has removed some impurities from original apatite ore.

3.1.4. Specific surface area.

By the BET method, the specific surface area of the apatite ore and purified apatite ore were determined using N₂ adsorption at 77 K. Figure 4 shows that the apatite ore sample has a lower adsorption capacity compared with the purified one. The specific surface area of purified apatite ore is 36.62 m²/g which is much higher than that of original apatite ore (3.76 m²/g). From the result it can be predicted that the purified apatite ore can adsorb better than the original apatite ore.

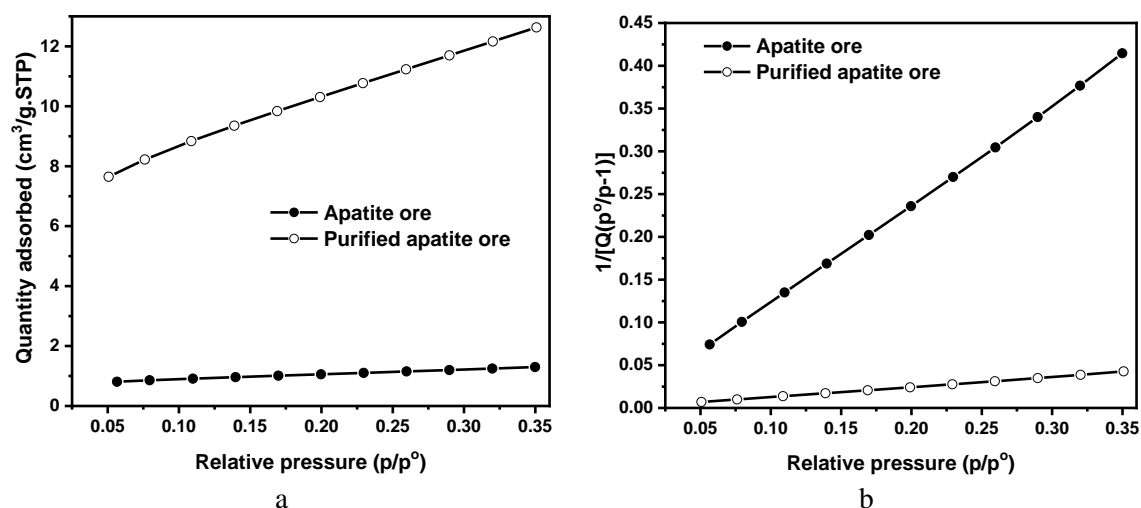


Figure 4. The N₂ adsorption isotherm (a) and BET plot (b) of apatite ore and purified apatite ore.

3.1.5. Energy-dispersive X-ray Spectroscopy.

Figure 5 and Table 1 show the composition and percentage of elements present in apatite ore and purified one. The data on apatite ore are consistent with the XRD results (Figure 3) and the company's published production criteria. The EDX spectra present characteristic peaks for main elements in apatite (Ca, P, O, F) and other metals with a small content such as Mg, Al, K, Mn, and Fe. The ratio of Ca/P in apatite ore and purified one is 1.51 and 1.60, respectively, as shown in Table 1. This value is close to that in Ca₁₀(PO₄)₆F₂ molecules (1.67).

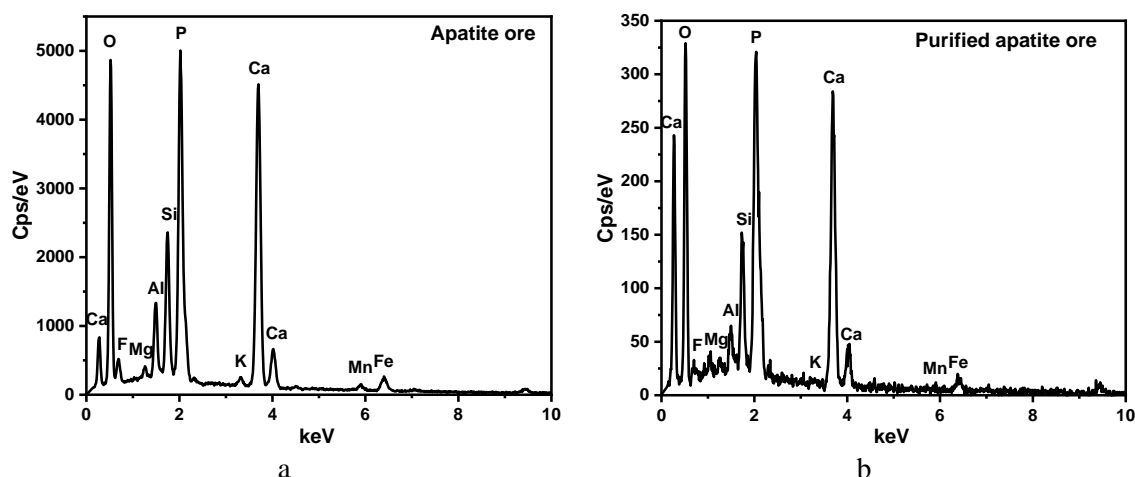


Figure 5. EDX spectrum of apatite ore (a) and purified apatite ore (b).

Table 1. The component of elements in apatite ore and purified apatite ore.

Element	Apatite ore		Purified apatite ore	
	% m	% a	% m	% a
O	51.14	68.74	55.98	73.27
Ca	20.62	11.06	20.91	10.82
P	10.53	7.31	10.12	6.76
F	2.98	3.37	2.39	2.63
Si	4.60	3.53	4.53	3.38
Al	4.14	3.30	1.56	1.21
Mn	0.88	0.35	0.48	0.18
Mg	0.46	0.41	0.45	0.39
K	0.89	0.49	0.08	0.04
Fe	3.74	1.44	3.50	1.31

3.2. Research on Pb^{2+} adsorption of apatite ore

3.2.1. Calibration curve of Pb^{2+}

Solutions with initial Pb^{2+} concentrations ranging from 0.25 - 3 mg/L were diluted from a 1000 mg/L solution. Forming a color complex with dithizone and measuring it with a UV-Vis spectrophotometer at 520 nm, we obtain the value of absorbance A. The variation of absorbance A with Pb^{2+} concentration is presented in Figure 6. Linear calibration curve ($y = 0.82513x$) with correlation coefficient $R^2 = 0.991$ was used to determine Pb^{2+} concentration in the next experiments.

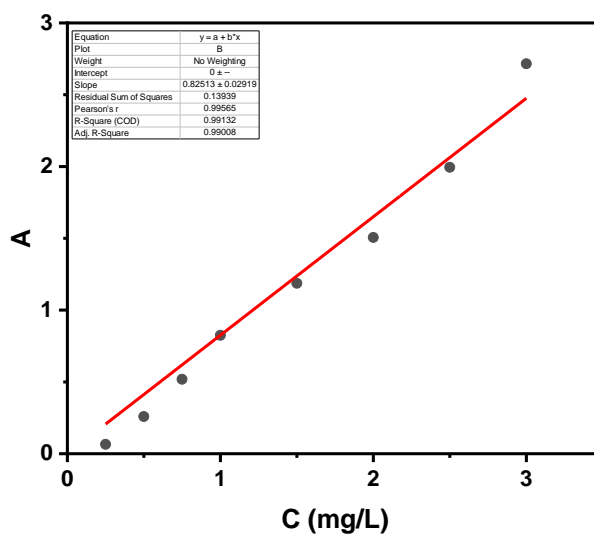


Figure 6. Variation of absorbance A against concentration C.

3.2.2. Effect of apatite mass.

Figure 7 shows the effect of adsorbent mass on adsorption capacity and efficiency. The residual concentration of Pb^{2+} in the solution decreases when the mass of apatite ore increases, leading to a rise in the efficiency and a reduction in the adsorption capacity. Specifically, when the apatite mass rises from 0.05 g to 0.15 g, the efficiency increases rapidly from 61.96 % to 86.31 %. After that, in the range of adsorbent mass from 0.2 to 0.3 g, the efficiency increases slowly as the adsorption is reaching equilibrium. So, to obtain high adsorption efficiency and capacity, 0.15 g is selected to be used for the next experiments.

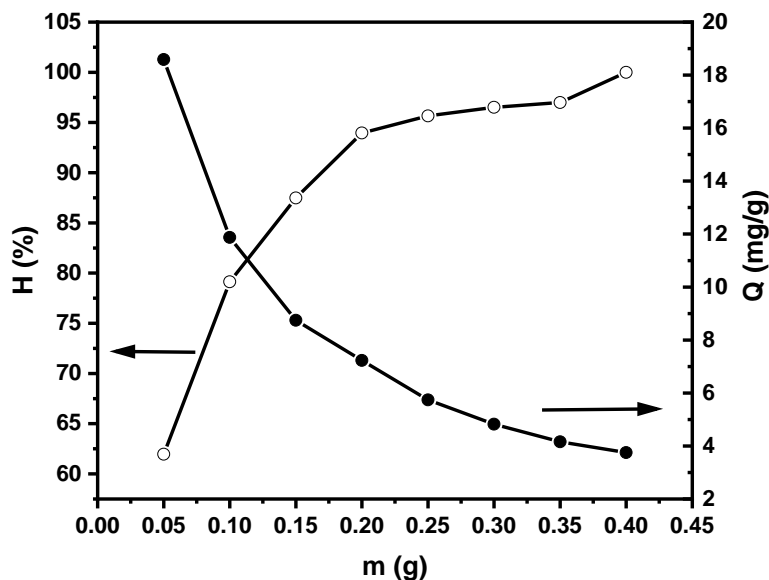


Figure 7. Variation of adsorption efficiency and capacity against mass of apatite ore (at pH_0 , $C_0 = 30$ mg/L, contact time = 45 minutes).

3.2.3. pH point zero charge (pH_{pzc}).

pH_{pzc} was determined according to the following procedure: 50 mL of 0.01 M KCl solution was adjusted to pH from 4 to 9 (pH_{before}) using 0.01 M HCl and 0.01 M KOH solutions. 0.15 g of apatite ore was dispersed in the above solution, which was then stirred for 45 minutes at a rate of 400 rpm at room temperature. The mixture was filtered and the obtained solution was measured for pH value (pH_{after}). pH_{pzc} was determined by the intersection point of the ΔpH curve ($\Delta pH = pH_{after} - pH_{before}$) against pH_{before} on the horizontal axis.

The result of specifying pH_{pzc} of apatite ore is presented in Figure 8. From Figure 8, the adsorbent material has $pH_{pzc} = 6.7$. Depending on the pH of the solution, the surface of the material has a negative or positive charge. If the adsorption process is conducted at solution pH $< pH_{pzc} = 6.7$, the surface of the material has a positive charge, and vice versa, at solution pH > 6.7 , the adsorbent's surface has a negative charge. From the pH_{pzc} value, the adsorption capacity of the material can be explained depending on the pH of the solution.

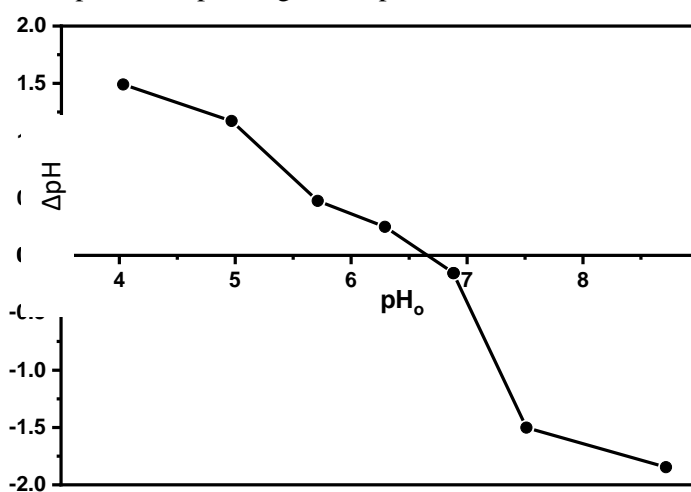


Figure 8. Graph for determining pH_{pzc} of apatite ore.

3.2.4. Effect of pH.

The Pb^{2+} adsorption process of apatite ore at different pH from 2.7 to 7.5 was performed and the results are presented in Figure 9. pH is one of the factors which directly affect the adsorption of heavy metal ions. The Pb^{2+} adsorption capacity and efficiency increase when solution pH increases from 2.7 to 7.5. With pH $< pH_{pzc} = 6.7$, the adsorption efficiency and capacity have maximum value at pH of solution $pH_0 = 5.4$. When pH is lower than pH_{pzc} , the surface of apatite ore has a positive charge, so the electrostatic force is the interactive force. In addition, if the concentration of H^+ ions is high, metal cations were competed by H^+ ions in the treatment process, leading to a decrease in the efficiency. In the case of pH higher than pH_{pzc} , the adsorption efficiency and capacity increase. This can be explained as follows: the surface of apatite ore has a negative charge at a high pH value, but the precipitation of $Pb(OH)_2$ could happen if the pH is too high. To make it easier for real applications, pH = $pH_0 = 5.4$ is used for future experiments.

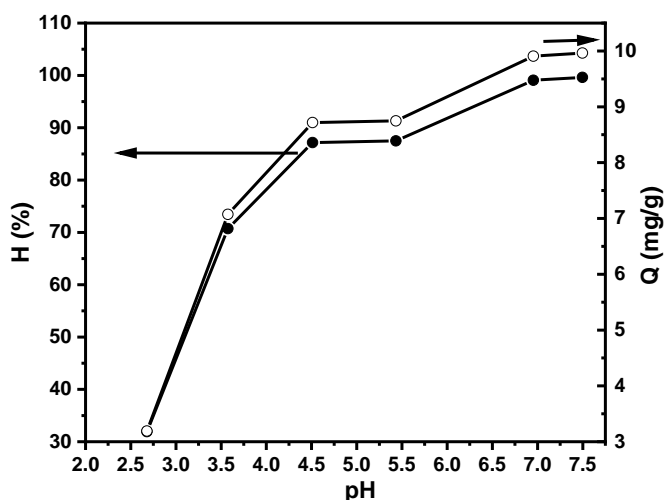


Figure 9. Variation of adsorption efficiency and capacity against pH with $m_{\text{apatite}} = 0.15\text{g}$, $C_0 = 30\text{mg/L}$, contact time = 45 minutes

3.2.5. Effect of contact time.

The adsorption process was investigated in the different contact times from 15 to 70 minutes. The results are presented in Figure 10. Contact time is also an important factor that has a great influence on the adsorption ability of apatite ore. When contact time increases from 15 to 60 minutes, the efficiency and capacity rise rapidly from 77.58 % to 94.03 % and from 7.76 mg/g to 9.4 mg/g, respectively. With contact time from 60 minutes to 70 minutes, the efficiency and capacity slowly rise. This can be explained as follows: as the contact time increases, more Pb^{2+} ions can be adsorbed in the pores of the apatite ore, so the adsorption capacity and efficiency rise. But at a certain time, when the adsorption process reaches equilibrium, metal ions are maximally adsorbed, so if the contact time continuously increases, the adsorption capacity is almost unchanged. Therefore, 60 minutes is a suitable contact time for apatite ore.

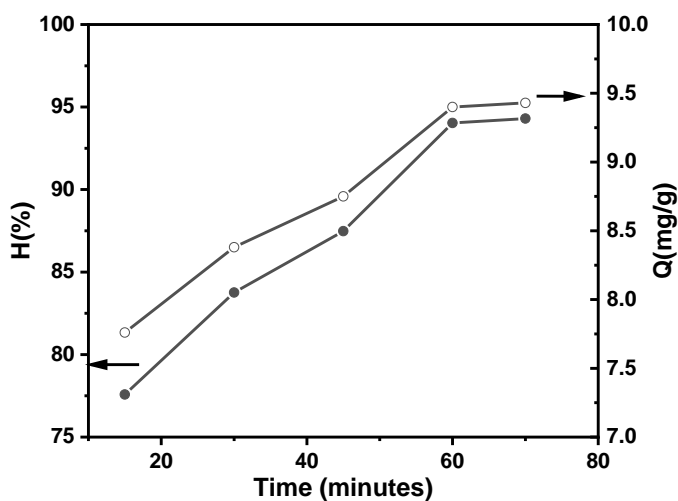


Figure 10. Variation of adsorption efficiency and capacity against contact time with $C_0 = 30\text{ mg/l}$, pH_0 , $m_{\text{apatite}} = 0.15\text{ g}$.

3.2.6. Adsorption kinetics.

The Pb^{2+} adsorption process on apatite ore was very complicated and it is hardly possible to determine the real kinetics of the adsorption process, so we can only use pseudo kinetic equations to describe the adsorption process. Therefore, we study the Pb^{2+} adsorption process on apatite ore according to the Lagergren's pseudo-first-order law, McKay and Ho's pseudo-second-order law, and the intra-particle diffusion model from the experimental data obtained after different time intervals from 15 to 70 minutes. The equations of three models are given in Eqs. (2), (3) and (4), respectively:

$$\ln(q_e - q_t) = \ln q_e - k_1 t \quad (2)$$

where q_t (mg/g) is the adsorption capacity at time t , q_e (mg/g) is the adsorption capacity at equilibrium, and k_1 (min^{-1}) is the pseudo-first-order adsorption rate constant;

$$\frac{t}{q_t} = \frac{1}{k_2 q_e^2} + \frac{1}{q_e} t \quad (3)$$

where k_2 ($\text{g}/\text{min} \cdot \text{mg}$) is the pseudo-second-order rate constant for adsorption; and

$$q_t = k_p t^{1/2} + C \quad (4)$$

where C is the intercept that shows the ideal boundary layer thickness and k_p is the intra-particle diffusion rate constant ($\text{mg}/\text{g} \cdot \text{min}^{1/2}$).

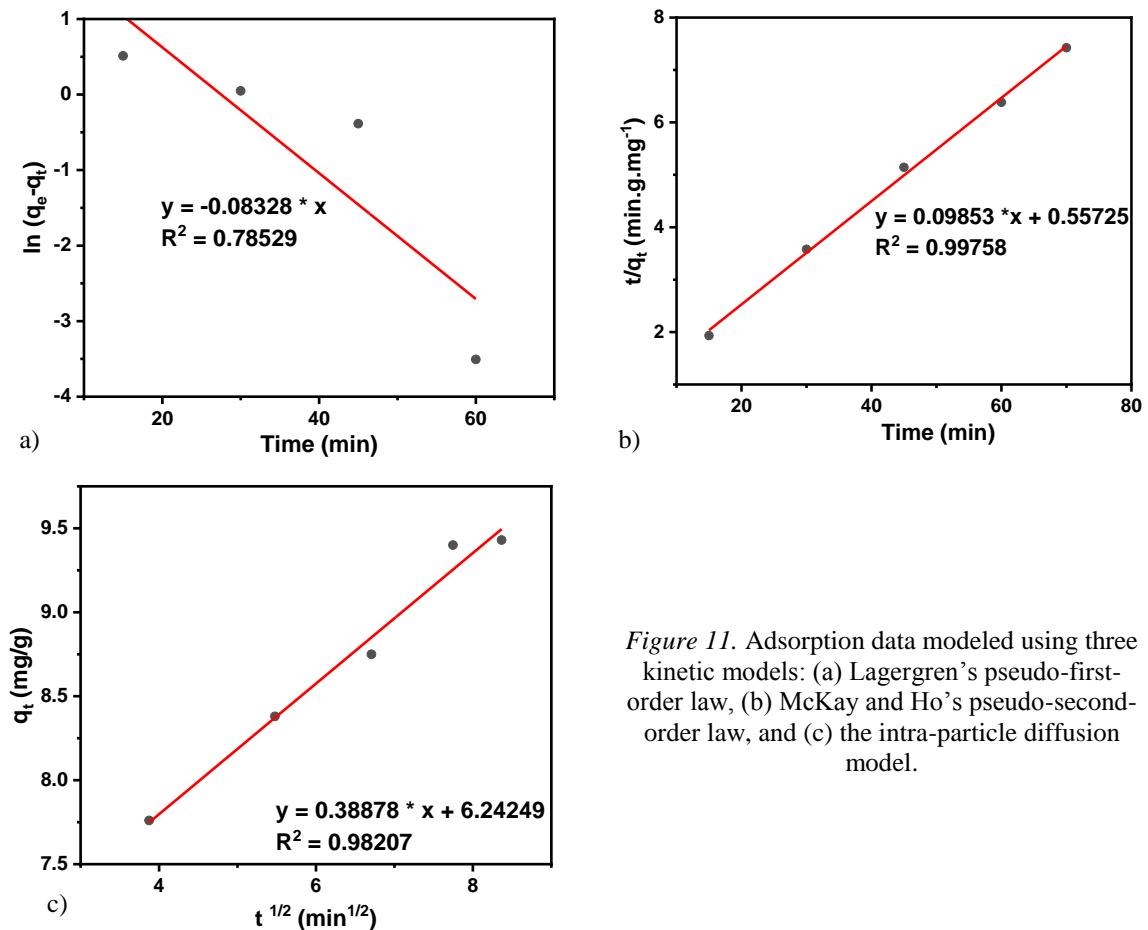


Figure 11. Adsorption data modeled using three kinetic models: (a) Lagergren's pseudo-first-order law, (b) McKay and Ho's pseudo-second-order law, and (c) the intra-particle diffusion model.

Table 2. Parameters of Pb^{2+} removal process calculated using McKay and Ho's pseudo-second-order law model.

k_2 (g/mg.min)	q_e (mg/g)	R^2
0.017	10.149	0.99758

Figure 11 presents the kinetic data plotted using Lagergren's pseudo-first-order equation (Eq. 2, Figure 11a), McKay and Ho's pseudo-second-order equation (Eq. 3, Figure 11b), and the intra-particle diffusion (Eq. 4, Figure 11c), respectively. A linear relationship with a high correlation coefficient ($R^2 = 0.99758$) between t/q_t and t was obtained, which indicates that the Pb^{2+} adsorption on apatite ore fitted the pseudo-second-order model better than other models. The calculated parameters of this model are given in Table 2.

3.2.6. Influence of initial Pb^{2+} concentration

When the initial Pb^{2+} concentration varies from 10 to 100 mg/L, the adsorption efficiency decreases and the capacity increases (Figure 12). But when the initial Pb^{2+} concentration rises to a certain value, the adsorption capacity nearly has no augmentation (corresponding to the adsorption process reaching the saturated state). This can be explained as follows: with a content of apatite ore corresponding to a certain number of adsorption pores, when all the adsorption pores are fully filled by Pb^{2+} ions, the adsorption capacity is almost unchanged even though the concentration of Pb^{2+} continuously increases.

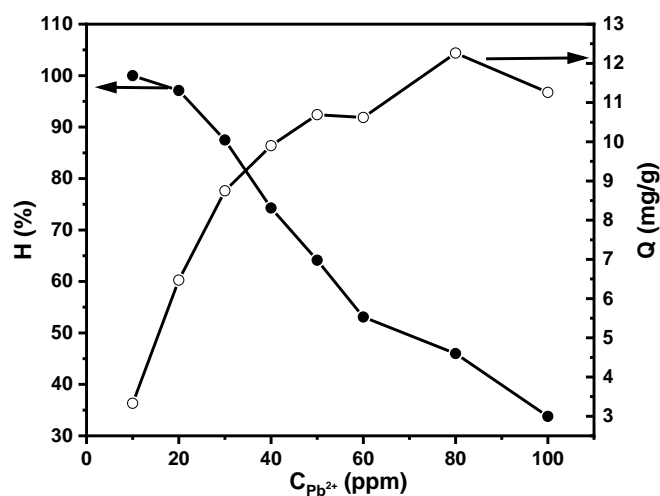


Figure 12. Variation of adsorption efficiency and capacity against Pb^{2+} ions initial concentration with $m_{\text{apatite}} = 0.15$ g, pH_0 , contact time = 60 minutes.

3.2.7. Maximum adsorption capacity

The Pb^{2+} adsorption process was conducted under the following conditions: 0.15 g of apatite with a contact time of 60 minutes at pH_0 and varying initial concentration of Pb^{2+} ion. The concentration of residual Pb^{2+} at equilibrium state (C_e) was then determined. From the experimental data, the parameters $\ln C_e$, C_0/Q_e , and $\ln Q_e$ were calculated, and Langmuir and Freundlich isotherm adsorption models were established. The results obtained are presented in

Figure 13, indicating that both adsorption isotherm models can be used to describe the experimental data of the Pb^{2+} adsorption process by apatite ore under research conditions. However, the Langmuir model ($R^2 = 0.99876$) is better than the Freundlich one ($R^2 = 0.99201$). From the isotherm curve, the Pb^{2+} maximum adsorption capacity Q_{max} was obtained with a value of 11.26 mg/g.

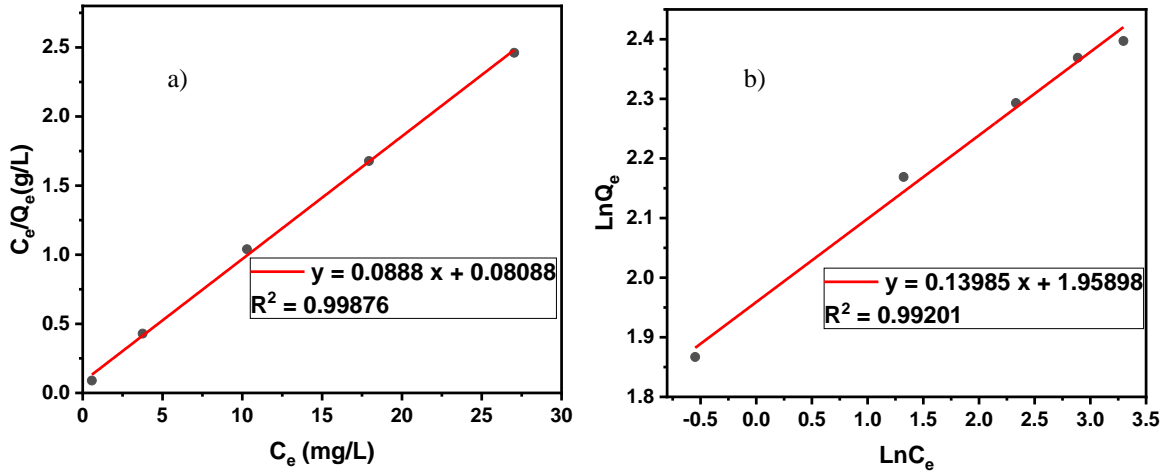


Figure 13. Adsorption isotherm curves of Pb^{2+} against the Langmuir model (a) and Freundlich (b)

3.2.8. XRD diffraction

Figure 14 shows the XRD patterns of apatite ore before and after Pb^{2+} adsorption. Similar peaks of the two materials were observed including the characteristic peaks of fluorapatite, SiO_2 , and calcium aluminum oxide. This result shows that the phase structure of apatite ore did not change after the adsorption, proving that the adsorption process is physical adsorption.

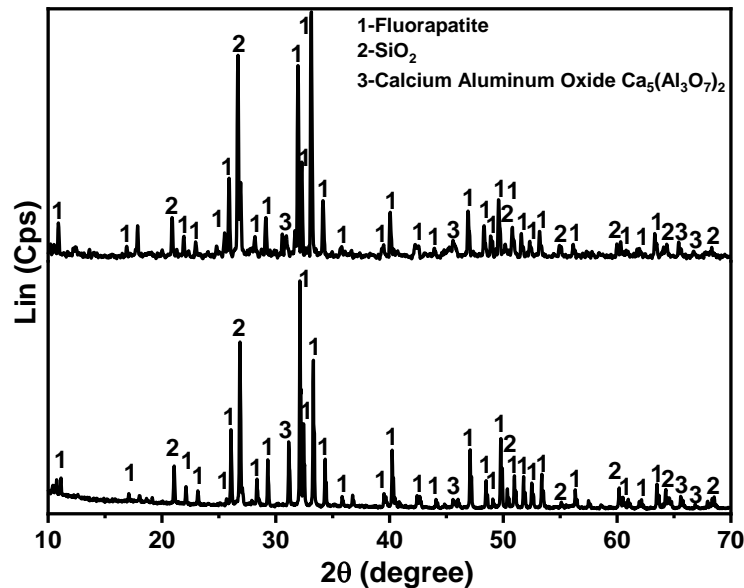


Figure 14. XRD patterns of apatite ore before and after Pb^{2+} adsorption.

3.2.9. Zeta potential

The zeta potential of apatite ore before and after Pb^{2+} adsorption was presented in Figure 15. The value of zeta potential of apatite ore was initially -40.3 mV and after adsorption, it was -40.4 mV. The shape of the zeta potential curves of the two samples is similar, the 3 peaks appearing corresponding to the 3 components of the materials are shown in the XRD results. The negative value of the zeta potential of apatite ore indicates that this material has a negative charge and therefore easily interacts with heavy metal cations, leading to a good adsorption capacity of this material.

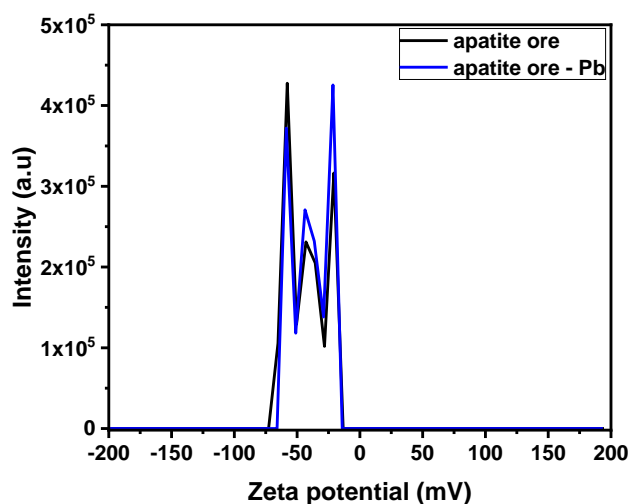


Figure 15. Zeta potential distribution of apatite ore before and after Pb^{2+} adsorption.

3.3. Comparison of Pb^{2+} adsorption ability of apatite ore and purified apatite ore

3.3.1. Calibration curve of Pb^{2+} by AAS method

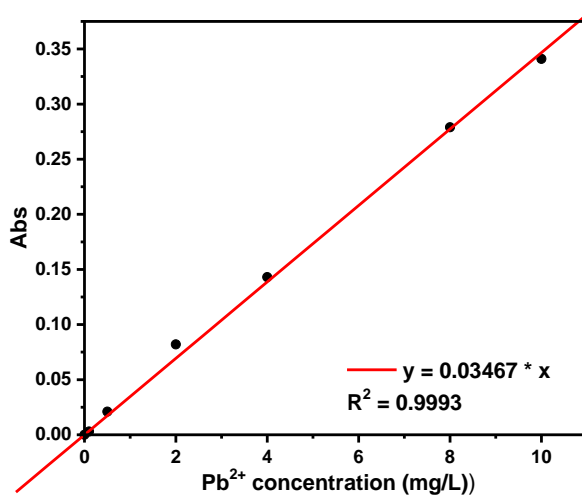


Figure 16. Calibration curve of Pb^{2+} determined by AAS method.

Solutions with an initial Pb^{2+} concentration of 0.1 to 10 mg/L were analyzed by AAS to obtain Abs values. The variation of the Abs values with Pb^{2+} concentration was shown in Figure 16. The calibration equation is a straight line: $y = 0.03467 * x$ with correlation coefficient $R^2 = 0.9993$, which was used to determine the concentration of Pb^{2+} in subsequent experiments.

3.3.2. Effect of adsorbent mass

Figure 17 presents the change of adsorption capacity and efficiency by mass of apatite ore (Figure 17.a) and purified apatite ore (Figure 17.b). With a mass of 0.15 g apatite ore, the adsorption yield after 45 minutes was about 75 %. For the purified ore, with a mass of 0.03 g and a contact time of 15 minutes, the adsorption efficiency was achieved at 90 % with a capacity of about 36 mg/g. The results show that purified apatite ore has Pb^{2+} treatment ability better than original apatite ore, which is consistent with the specific surface area data (BET) in part 3.1.4.

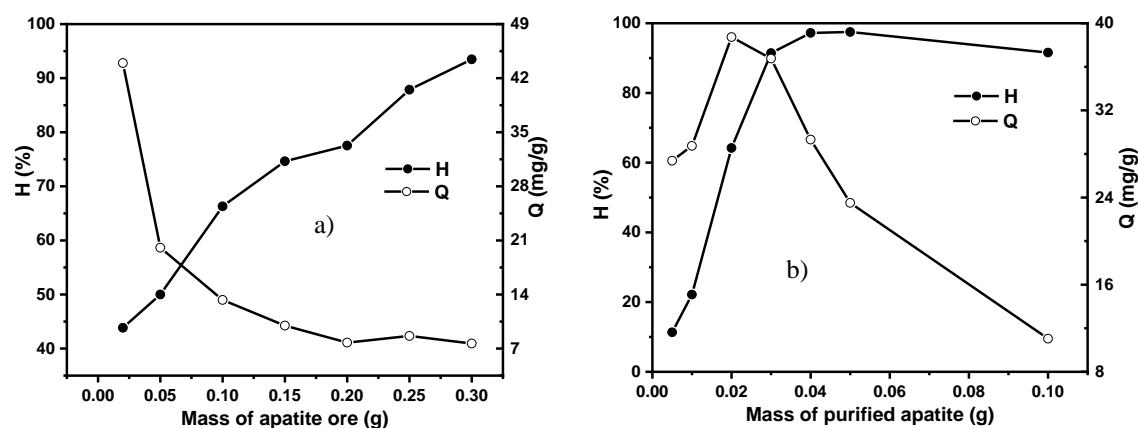


Figure 17. Variation of adsorption capacity (Q) and efficiency (H) against mass of apatite ore (a) and purified apatite ore (b) at $C_o = 30$ mg/L, pH_o , $t = 45$ minutes with apatite ore and 15 minutes with purified apatite ore.

4. CONCLUSIONS

Apatite ore, the main component of which is fluorapatite, has a specific surface area of 3.76 m^2/g , the grain size is not uniform, the large particles can reach $15-20$ μm , the smallest particle size is about 200 nm. After purification, the specific surface area increased to 36.62 m^2/g , the particles are smaller and more uniform in size. Suitable conditions for treating Pb^{2+} with apatite ore are as follows: 0.15 g of mass adsorbent, natural pH of the solution, contact time of 60 minutes. The adsorption process follows the Langmuir isotherm model with a maximum capacity of 11.26 mg/g and the kinetic data of the adsorption process fitted the pseudo-second-order model better than other models. The purified apatite ore can adsorb Pb^{2+} better than the original apatite ore.

Acknowledgements. This research was funded by the Institute for Tropical Technology (ITT), Vietnam Academy of Science and Technology (VAST) with grant no. VAST07.02/20-21.

Credit authorship contribution statement. Nguyen Thu Phuong: Methodology, Formal analysis, Funding acquisition. Cao Thi Hong: Investigation, Formal analysis. Nguyen Thi Thuy: Investigation, Formal analysis. Nguyen Thi Xuyen: Investigation, Formal analysis. Nguyen Thi Thom: Formal analysis. Pham

Thi Nam: Formal analysis. Nguyen Thi Thu Trang: Formal analysis. Do Thi Hai: Formal analysis. Dinh Thi Mai Thanh: Supervision

Declaration of competing interest. The authors declare that they have no known competing financial interests or personal relationships that could have appeared to influence the work reported in this paper.

REFERENCES

1. Hong P. T., Anh D. T. N., Nha D. T., Hai D. H and Huong H. T. T. - Metal bioaccumulation in fishes and macro zooplankton in some lakes in Hanoi, Vietnam J. Sci. Technol. **56** (2C) (2018) 96-103. <https://doi.org/10.15625/2525-2518/56/2C/13035>.
2. Hong P. T., Ha L. T. T., Hien N. T. T., Chung N. T., Hung N. Q., Cuong N. C. and Huong H. T. T. - Combination impact of pH and temperature on the toxicity of lead on zooplankton in the context of global warming, Vietnam J. Sci. Technol. **58** (5A) (2020) 105-114. <https://doi.org/10.15625/2525-2518/58/5A/15214>.
3. Rupa C., Anupama A., Ajaya K. S., Bhawana J. and Abu B. H. S. - Adsorption of heavy metal ions by various low-cost adsorbents: a review, Int. J. Environ. Anal. Chem. (2020). <https://doi.org/10.1080/03067319.2020.1722811>.
4. Anh N. D. - Study on synthesis of MnFe₂O₄/GNPs composite and application on heavy metal removal, Vietnam J. Sci. Technol. **56** (1A) (2019) 204-211. <https://doi.org/10.15625/2525-2518/56/1A/12524>.
5. Shraddha P., Srinivas M K., Raja S. and Arivalagan P. - A review on the synthesis of hydroxyapatite, its composites and adsorptive removal of pollutants from wastewater, J. Water Process Eng. **38** (2020) 101574. <https://doi.org/10.1016/j.jwpe.2020.101574>.
6. Phuong V. T., Nam P. T., Phuong N. T., Hai D. T. and Thanh D. T. M. - Defluoridation behavior of nano Zn-hydroxyapatite synthesized by chemical precipitation method, Vietnam J. Chem. **50** (6B) (2012) 239-244.
7. Duyen L. T., Thao L. T. P., Hai D. T., Hanh V. T., Nam P. T., Thom N. T., Hong C. T., Phuong N. T., Thanh D. T. M., Hai L. V. et al. - Fabrication of porous hydroxyapatite granules as an effective adsorbent for the removal of aqueous Pb(II) ions, J. Chem. **2019** (2019) 8620181. <https://doi.org/10.1155/2019/8620181>.
8. Phuong N. T., Xuyen N. T., Trang N. V., Thom N. T., Thai V. Q., Huy N. T., Nam P. T., Thanh D. T. M. - Treatment of Cd²⁺ and Cu²⁺ ions using modified apatite ore, J. Chem. **2020** (2020) 652197. <https://doi.org/10.1155/2020/652197>.
9. Thom N. T., Thanh D. T. M., Nam P. T., Phuong N. T. and Claudine B-H. - Adsorption behavior of Cd²⁺ ions using hydroxyapatite (HAp) powder, Green Process. Synth. **7** (5) (2018) 409-416. <https://doi.org/10.1515/gps-2018-0031>.
10. Bostick W.D., Jarabek R.J. and Conca J.L. - Phosphate-Induced Metal Stabilization: Use of Apatite and Bone Char for the Removal of Soluble Radionuclides in Authentic and Simulated DOE Groundwater, Proceedings of the Air and Waste 92nd Annual Meeting and Exhibition, St. Louis, MO, USA, 1999.
11. Bostick W. D. - Use of apatite for chemical stabilization of subsurface contaminants, Final Report of Contract: DE-AC26-01NT41306 of U.S. Department of Energy, National Energy Technology Laboratory, New York, NY, USA, 2003.

12. Martinez R. J., Beazley M. J. and Sobecky P. A. - Phosphate-mediated remediation of metals and radionuclides, *Advances in Ecology*, **2014** (2014) 786929. <https://doi.org/10.1155/2014/786929>.
13. Conca J. L., Lu N., Parker G., Moore B. and Adams A. - PIMS – remediation of metal contaminated waters and soils, *Proceedings of the Second International Conference on Remediation of Chlorinated and Recalcitrant Compounds*, May (2000) with an Addendum from ICAM, Monterey, CA, USA, 2000.
14. Thomson B. M., Smith C. L., Busch R. D., Siegel M. D. and Baldwin C. - Removal of metals and radionuclides using apatite and other natural sorbents, *J. Environ. Eng.* **129** (6) (2003) 492-499. [https://doi.org/10.1061/\(ASCE\)0733-9372\(2003\)129:6\(492\)](https://doi.org/10.1061/(ASCE)0733-9372(2003)129:6(492)).
15. Basta N. T. and McGowen S. L. - Evaluation of chemical immobilization treatments for reducing heavy metal transport in a smelter-contaminated soil, *Environ. Pollut.* **127** (1) (2004) 73-82. [https://doi.org/10.1016/S0269-7491\(03\)00250-1](https://doi.org/10.1016/S0269-7491(03)00250-1).
16. James C. - Phosphate – Induced Metal Stabilization, Report of Contract: 68D60023 of United States Environmental Protection Agency, 1997.
17. Wang J., Chao Y., Wan Q., Zhu Z. and Yu H. - Fluoridated hydroxyapatite coatings on titanium obtained by electrochemical deposition, *Acta Biomater.* **5** (5) (2009) 1798–1807. <https://doi.org/10.1016/j.actbio.2009.01.005>.
18. Nikčević I., Jokanović V., Mitrić M., Nedić Z., Makovec D. and Uskoković D. - Mechanochemical synthesis of nanostructured fluorapatite/ fluorhydroxyapatite and carbonated fluorapatite/ fluorhydroxyapatite, *J. Solid State Chem.* **177** (2004) 2565–2574. <https://doi.org/10.1016/j.jssc.2004.03.024>.
19. Hang D. T. T. and Chi D. K. - Removal of heavy metal from industrial water by apatite mineral, *Vietnam J. Sci. Technol.* **72A** (2009) 83-87.
20. Van M. D., Huu T. V., Hoa T. M. D., Duy H. N., Huan-Ping C., Lan H. N. and Chu-Ching L. - Evaluation of fly ash, apatite and rice straw derived-biochar in varying combinations for in situ remediation of soil contaminated with multiple heavy metals, *Soil Sci. Plant Nutr.*, **66** (2) (2020) 379-388. <https://doi.org/10.1080/00380768.2020.1725913>.
21. Viet N. T. M., Hoa N. T. - Study on adsorption capacity of methylene blue and phenol red on Lao Cai apatite ore, *J. Anal. Sci.* **22** (2) (2017) 124-131.
22. Viet N. T. M., Yen L. T. H. – Investigation of adsorption capacity of Mn(II), Ni(II) on Lao Cai apatite ore modified by acid, *Vietnam J. Chem.* **54** (5e1,2) (2016) 97-101.